

## Solutol HS15 based binary mixed micelles with penetration enhancers for augmented corneal delivery of sertaconazole nitrate: optimization, *in vitro*, *ex vivo* and *in vivo* characterization

Nihal Farid Younes , Sally Adel Abdel-Halim and Abdelhalim I. Elassasy

Department of Pharmaceutics and industrial pharmacy, Faculty of pharmacy, Cairo University, Cairo, Egypt

### ABSTRACT

Keratomycolysis is a serious corneal disease that can cause a permanent visual disability if not treated effectively. Sertaconazole nitrate (STZ), a novel broad spectrum antifungal drug, was suggested as a promising treatment. However, its utility in the ocular route is restricted by its poor solubility, along with other problems facing the ocular delivery like short residence time, and the existing corneal barrier. Therefore, the objective of this study was to formulate STZ loaded binary mixed micelles (STZ-MMs) enriched with different penetration enhancers using thin-film hydration method, based on a  $3^{1.2^2}$  mixed factorial design. Different formulation variables were examined, namely, type of auxiliary surfactant, type of penetration enhancer, and total surfactants: drug ratio, and their effects on the solubility of STZ in MMs ( $S_M$ ), particle size (PS), polydispersity index (PDI), and zeta potential (ZP) were evaluated. STZ-MMs enhanced STZ aqueous solubility up to 338.82-fold compared to free STZ. Two optimized formulations (MM-8 and MM-11) based on the desirability factor (0.891 and 0.866) were selected by Design expert<sup>®</sup> software for further investigations. The optimized formulations were imaged by TEM which revealed nanosized spherical micelles. Moreover, they were examined for corneal mucoadhesion, stability upon dilution, storage effect, and *ex vivo* corneal permeation studies. Finally, both *in vivo* corneal uptake and *in vivo* corneal tolerance were investigated. MM-8 showed superiority in the *ex vivo* and *in vivo* permeation studies when compared to the STZ-suspension. The obtained results suggest that the aforementioned STZ loaded mixed micellar system could be an effective candidate for Keratomycolysis-targeted therapy.

### ARTICLE HISTORY

Received 28 May 2018  
Revised 30 June 2018  
Accepted 2 July 2018

### KEYWORDS

Sertaconazole nitrate; mixed micelles; Keratomycolysis; corneal permeability; confocal laser scanning

### Introduction

Keratomycolysis is a severe inflammation of the layers of the cornea caused by fungal invasion, associated with sudden onset of pain, sensitivity to light, secretions, corneal ulcers, and blurred vision (Ansari et al., 2013). Keratomycolysis can cause serious damages compared to other types of keratitis (bacterial or viral), which can be irreversible and finally results in loss of vision if not treated effectively (Prajna et al., 2013).

Topical antifungals, especially those formulated as eye-drops are the cornerstone for keratomycolysis treatment (Al-Badriyeh et al., 2010; Fernández-Ferreiro et al., 2016), yet their efficacy is limited by the several anatomical and physiological protective barriers of the human eye, such as the tight junctions of the corneal epithelium, mucoaqueous layer, tear turnover, blinking of the eye, and the nasolachrymal drainage (Nettey et al., 2016; Imam et al., 2017). Accordingly, the design of new nano-systems capable of conveying anti-fungal drugs at suitable therapeutic concentrations to their target ocular tissue has become inevitable for the continuous

development of the ocular pharmaceutical industry (Kaur et al., 2008; Higa et al., 2013).

Sertaconazole nitrate (STZ) is a new antifungal agent of the imidazole class with antifungal activity against wide range of pathogenic fungi, some of which are *Fusarium*, *Aspergillus*, and yeasts (Croxtall and Plosker, 2009), which are the most common contributory factors for fungal ocular diseases (He et al., 2016). STZ is reported to have good ocular tolerance (Romero et al., 1996), which makes it an excellent candidate for the treatment of keratomycolysis. However, the extreme poor aqueous solubility of STZ acts as an obstacle that limits its ocular clinical efficacy (Albet et al., 1992), and urges for the development of new delivery systems capable of enhancing its aqueous solubility, and improving its ocular penetration and retention.

Recently, mixed micellar systems created by the assembly of two or more surfactants have gained an increasing interest as a promising nanotechnology-based ocular drug delivery system (Mandal et al., 2017). They have a core/shell structure that is capable of harboring drugs with poor aqueous solubility within its hydrophobic core through

hydrophobic interactions (Aliabadi and Lavasanifar, 2006). The synergistic effect of the mixture of surfactants leads to an improved performance if compared to single surfactant micelles (Ribeiro et al., 2012). Mixed micelles have the advantages of large drug loading capacity, biodegradability, non-irritancy, ability to control drug release, unique thermodynamic stability in physiological solutions, and the ease of scaling up to industrial scale (Lu and Park, 2013; Yokoyama, 2014). They have also been reported to deliver poorly water soluble drugs to the target ocular tissue at suitable therapeutic concentrations following topical administration through enhancement of the corneal permeability/retention, as in itraconazole (Jaiswal et al., 2015), cyclosporine A (Grimaudo et al., 2018), curcumin (Duan et al., 2015a), and others.

Solutol<sup>®</sup> HS-15 (HS15), a nonionic surfactant, comprised of 70% of polyglycol mono- and di-esters of 12-hydroxystearic acid and 30% of free polyethylene glycol (Hou et al., 2016). It is characterized by its high stability, good biocompatibility, enhanced mucosal permeability, excellent solubilization power of hydrophobic drugs, and the ability to alter the pharmacokinetics of many drugs (Alani et al., 2010; Shubber et al., 2015). The past few years have witnessed the use of HS15 in the development of several ocular drug delivery systems, these systems were investigated and found to have promising outcomes regarding either corneal permeability or corneal retention (Gan et al., 2009; Chen et al., 2013).

The use of penetration enhancers is another way to improve the bioavailability and the therapeutic response of topical ophthalmic drugs. They can temporarily modulate the integrity of the corneal epithelium, thus promoting the transcorneal penetration of drugs (Kaur and Smitha, 2002). In order for a penetration enhancer to be used in ophthalmic preparations, it should cause no toxicological complications, preserve the functionality of ocular tissue and have minimal irritation effect (Chetoni et al., 2003). Several penetration enhancers were included in ocular delivery systems and showed a significant effect on corneal permeability, as for example, Ethylenediaminetetraacetic acid, sodium glycolate, Borneol, and Brij<sup>®</sup> 78 (Mahaling and Katti, 2016; Mehta et al., 2017).

Literature offers limited data about the use of STZ in an ocular drug delivery system. Thus, this work aims firstly to enhance the aqueous solubility of STZ through loading into Solutol<sup>®</sup> HS15 based mixed micelles enriched with penetration enhancers. A 3<sup>1</sup>.2<sup>2</sup> mixed factorial design was employed to study the influence of different formulation variables on the mixed micelles' characteristics and to elucidate the optimized formulations. Secondly, several tests were done to evaluate the efficacy of the optimized formulations in the ocular delivery, such as mucoadhesion, stability upon dilution, *ex vivo* corneal permeation, *in vivo* ocular tolerance, and *in vivo* ocular uptake.

## Materials and methods

### Materials

STZ was supplied as a kind gift by October Pharma, 6th of October City, Egypt. Solutol<sup>®</sup> HS 15 (**HS15**), Pluronic<sup>®</sup> F68

(**F68**), Brij<sup>®</sup> 58 (**B58**), Pluronic<sup>®</sup> L121 (**L121**), and Rhodamine B (**RhB**) were purchased from Sigma-Aldrich<sup>®</sup> Inc. AL, USA. Transcutol<sup>®</sup> P (**Trc**) was supplied as a gift by Gattefossé, France. Propylene glycol (**PG**), ethanol (95%), sodium bicarbonate, sodium chloride, and calcium chloride were purchased from Adwic, El-Nasr Pharmaceutical Chemicals Co., Cairo, Egypt. All other chemicals and solvents were of analytical grade and used without further purification. The water used was deionized, distilled water.

### Animals

This study followed the Association for Research in Vision and Ophthalmology resolution on the use of animals in ophthalmic research. In addition, Animal ethics clearance was attained from the Ethical Committee of Faculty of Pharmacy, Cairo University (approval number **PI 2132**). Adult male New Zealand albino rabbits weighing 2–3 kg were used in this study. The animals were housed in separate cages in a ventilated light-controlled room (12-h light and 12-h dark cycles) at 25 ± 2 °C with free access to food and water. All animals were in good health and have no clinically observed abnormalities. At the end of each experiment, the animals were euthanized by decapitation after anesthetizing them by intramuscular injection of 35 mg/kg Ketamine and 5 mg/kg Xylazine, the bodies and the remains of rabbits were frozen till incinerated.

### Experimental factorial design

STZ loaded mixed micelles (STZ-MMs) were prepared using a 3<sup>1</sup>.2<sup>2</sup> mixed factorial design. The factors studied were; type of auxiliary surfactant (A) at 3 levels (L121, B58, and F68), type of penetration enhancer (B) at 2 levels (Trc and PG), and total surfactants: drug ratio (C) at 2 levels (10:1 and 20:1 w/w). The responses studied were; solubility of STZ in MMs ( $S_M$ ), particle size (PS), polydispersity index (PDI), and zeta potential (ZP) ( $Y_1$ ,  $Y_2$ ,  $Y_3$ , and  $Y_4$ , respectively). The factors studied with their respective levels and the responses with their required constraints, together with detailed composition of the resultant formulations are shown in (Table 1).

### Preparation of STZ-MMs

STZ-MMs were prepared by thin-film hydration method (Yan et al., 2016; Fares et al., 2018). In brief, a binary mixture of surfactants (HS15 with L121, B58, or F68) were added to STZ (40 mg) at different weight ratios (10:1 and 20:1), along with 25 mg of either (Trc or PG) as a penetration enhancer. They were all co-dissolved in methanol (2.5 mL) by the ultrasonic method in a 500 mL round bottom flask. The solvent was then evaporated under reduced pressure using a rotary vacuum evaporator (Heidolph VV 2000, Burladingen, Germany) at 60 °C and 120 rpm, until a thin dry film was formed on the flask wall. The dried film was then hydrated using 5 mL distilled water under normal pressure at 60 °C and 120 rpm for 30 minutes. Afterwards, the prepared STZ-MMs were incubated at 25 ± 2 °C for 48 h then filtered through 0.22 μm

**Table 1.** Independent variables with the respective levels investigated in the 3<sup>1</sup>.2<sup>2</sup> mixed factorial design and the dependent variables with their required constraints, together with the detailed Composition of the prepared STZ-MMs formulations and their characterization.

Factors (independent variables)		Levels									
A: Auxiliary surfactant type	L121	B58	F68								
B: Penetration enhancer type	Trc	PG									
C: Total surfactants :drug ratio	10:1	20:1									
Responses (dependent variables)				Constraints							
Y <sub>1</sub> : S <sub>M</sub> (mg/mL)				Maximize							
Y <sub>2</sub> : PS (nm)				Minimize							
Y <sub>3</sub> : PDI				Minimize							
Y <sub>4</sub> : ZP (mV)				Maximize							
Formula	Factors' levels			S <sub>M</sub> (mg/mL)	F <sub>s</sub>	SI	PS (nm)	PDI	ZP (mV)		
	A	B	C								
MM-1	L121	Trc	10:1	2.56 ± 0.06	111.20	0.32	26.81 ± 0.29	0.302 ± 0.02	19.50 ± 0.57		
MM-2	B58	Trc	10:1	5.17 ± 0.50	224.80	0.65	19.09 ± 0.67	0.315 ± 0.03	33.63 ± 4.07		
MM-3	F68	Trc	10:1	2.02 ± 0.10	87.62	0.25	22.44 ± 2.14	0.415 ± 0.03	17.88 ± 0.32		
MM-4	L121	PG	10:1	2.51 ± 0.05	109.22	0.31	26.87 ± 1.05	0.334 ± 0.05	15.85 ± 1.77		
MM-5	B58	PG	10:1	5.40 ± 0.97	234.89	0.68	19.36 ± 0.10	0.360 ± 0.03	36.89 ± 2.81		
MM-6	F68	PG	10:1	1.99 ± 0.23	86.57	0.25	23.51 ± 0.08	0.380 ± 0.01	25.15 ± 0.78		
MM-7	L121	Trc	20:1	5.19 ± 0.32	225.60	0.65	21.25 ± 1.22	0.264 ± 0.01	30.25 ± 0.92		
MM-8	B58	Trc	20:1	7.79 ± 0.17	338.82	0.97	15.87 ± 0.71	0.249 ± 0.04	28.95 ± 4.38		
MM-9	F68	Trc	20:1	3.39 ± 0.13	147.55	0.42	18.61 ± 0.06	0.252 ± 0.00	22.55 ± 0.42		
MM-10	L121	PG	20:1	4.60 ± 0.26	200.17	0.58	21.67 ± 0.52	0.217 ± 0.01	18.28 ± 1.38		
MM-11	B58	PG	20:1	7.59 ± 0.16	329.91	0.95	16.39 ± 0.04	0.234 ± 0.04	23.33 ± 1.17		
MM-12	F68	PG	20:1	3.45 ± 0.14	149.91	0.43	19.20 ± 0.20	0.279 ± 0.05	15.25 ± 0.78		

Data are represented as (mean ± SD). S<sub>M</sub>: solubility of STZ in MM; F<sub>s</sub>: solubility factor; SI: stability index; PS: particle size; PDI: polydispersity index; ZP: zeta potential.

nylon membrane filter to remove the non-incorporated STZ, clear STZ-MMs were obtained (Chen et al., 2013).

$$SI = 1 - \frac{S_T - S_M}{S_M} \quad (2)$$

#### Determination of critical micelle concentration (CMC)

The CMC of single surfactants (HS15, L121, B58, and F68) and binary mixture of surfactants at weight ratio (1:1) (HS15/L121, HS15/B58, and HS 15/F68) were determined using the iodine (I<sub>2</sub>) UV spectroscopy method (Wei et al., 2009). Amounts of 1 g I<sub>2</sub> and 2 g potassium iodide (KI) were dissolved in 100 mL distilled water to prepare the KI/I<sub>2</sub> standard solution. Solutions of single/mixed surfactants with concentrations ranging from 0.00001% to 0.5% were prepared, an aliquot of 100 µL of KI/I<sub>2</sub> standard was added to each solution. The mixtures were incubated for 12 h in a dark place at 25 °C, after which the UV absorbance was measured at 366 nm (Shimadzu UV-1601PC, Kyoto, Japan). For CMC determination, the absorbance was plotted against the logarithm of surfactant concentration. The concentration, at which sharp increase in absorbance was recorded and considered as the CMC.

#### In vitro characterization of the prepared STZ-MMs

##### Solubility factor (F<sub>s</sub>) and stability index (SI)

Aliquots of filtered STZ-MMs, obtained just after preparation and also after 48 h incubation, were properly diluted with ethanol and analyzed spectrophotometrically at λ<sub>max</sub> 302.4 nm (Shimadzu UV-1601PC, Kyoto, Japan). Solubility factor (F<sub>s</sub>) and Stability index (SI) were calculated by the following equations.

$$F_s = \frac{S_M}{S_W} \quad (1)$$

Where S<sub>M</sub>, solubility of STZ in MM after 48 h; S<sub>W</sub>, solubility of STZ in distilled water (0.023 mg/ml); and S<sub>T</sub>, solubility of STZ in MM just after preparation.

##### Determination of PS, PDI, and ZP

The mean PS, PDI, and ZP of STZ-MMs were determined based on dynamic light scattering and electrophoretic mobility principles by Zetasizer Nano-ZS (Malvern Instrument Ltd., Worcestershire, UK) at 25 °C. Aliquots of samples were properly diluted with filtered deionized water to attain proper scattering intensity.

##### Testing the validity of the suggested models and selection of optimized STZ-MMs

In order to verify the performance of the fitted regression models; all measured values (actual values) for each response of the twelve suggested design points were compared to the predicted values using % deviation (Huang et al., 2004):

$$\% \text{ deviation in response } Y_m = 100|Y_{m\text{predicted}} - Y_{m\text{actual}}|/Y_{m\text{predicted}} \quad (3)$$

Additionally, to ascertain the validity of the suggested models, the 95% two-sided prediction intervals (95% PIs) for the predicted values were calculated and all measured values for each response were assessed to find whether they fall within the 95% PIs or not (Habib and AbouGhaly, 2016). Desirability function approach (DF) was applied by the Design<sup>®</sup> expert software in order to simultaneously compromise the several conflicting response variables to attain optimum

formulations that best satisfy the predetermined constraints previously listed in Table 1 (Park and Park, 1998).

### Differential scanning calorimetry (DSC)

DSC studies were carried out on STZ powder, HS15, B58, lyophilized plain optimized formulations, lyophilized STZ-loaded optimized formulations, and their physical mixtures using a differential scanning calorimeter (DSC-50, Shimadzu, Japan). The samples were accurately weighed (5 mg), hermetically sealed in aluminum pans and heated at a constant rate of 10 °C/min over the range of 20–250 °C. Sealed empty aluminum pan was used as a reference. Dry nitrogen gas was used as carrier gas with flow rate of 50 mL/min.

### Transmission electron microscopy (TEM)

After proper dilution, one drop of each of the optimized STZ-MMs formulations was placed over a carbon-coated copper grid. Then, it was negatively stained by adding one drop of 2% w/v phosphotungstic acid. After air drying of the stained samples, they were visualized using transmission electron microscope (JEM-1230; JEOL, Tokyo, Japan) operating at 80 kV.

### Mucoadhesion studies

Each of optimized STZ-MMs were mixed with 0.1% w/w aqueous mucin solution (1:40) and incubated at 37 ± 2 °C for 24 h at 100 rpm. At three different time points (6, 12, and 24 h), the PS and ZP of the dispersions were measured as mentioned previously. Also, the turbidity of the incubated dispersions was evaluated by measuring the transmittance % (T%) spectrophotometrically at  $\lambda_{\text{max}}$  500 nm (Shimadzu UV-1601PC, Kyoto, Japan) (Di Prima et al., 2017). The turbidity was calculated according to the following equation (Abdelbary and Tadros, 2013):

$$\text{Turbidity} = \frac{(100 - T\%)}{100} \quad (4)$$

Results were compared with ZP, PS, and turbidity values measured for mucin solution and aqueous MMs dispersions.

### Stability upon dilution

So as to mimic micellar dilution with lacrimal fluid after ocular administration, 30  $\mu\text{L}$  aliquot of each of the optimized formulations was placed into quartz cells containing simulated tear fluid (2970  $\mu\text{L}$ ) at 35 °C. The absorbance was registered spectrophotometrically at  $\lambda_{\text{max}}$  302.4 nm (Shimadzu UV-1601PC, Kyoto, Japan) every 60 s for a total time of 30 min (Alvarez-Rivera et al., 2016).

### Ex-vivo corneal permeation

*Ex vivo* corneal permeation experiments were performed using rabbit corneas (excised from eye globes after euthanizing the rabbits according to the guidelines stated before)

and a modified Franz diffusion cell with a diffusion area of 0.57 cm<sup>2</sup>. The corneas were softly rinsed with saline and inspected for being intact without wrinkles or pores, then it was mounted in the middle between the donor and the receptor compartments. The cells were kept at a constant temperature (35 ± 2 °C) and were magnetically stirred at 100 rpm through the whole experiment time. Each of the optimized STZ-MMs and STZ suspension (all equivalent to 5 mg) was placed in the donor compartment on the cornea and the receptor medium was 10 mL of freshly prepared simulated lacrimal fluid (pH 7.4) containing 2% sodium lauryl sulfate (to maintain sink condition). Aliquots of the medium (0.5 mL) were withdrawn at predetermined time intervals (0.5, 1, 2, 3, 4, 6, 8, 10, 12, and 24 h) replaced with the same volume of fresh medium to maintain a constant volume. The experiments were repeated three times and the mean ± SD was calculated. The concentration of STZ in the withdrawn samples was determined using HPLC (Shimadzu, Kyoto, Japan) equipped with an isocratic pump and a reversed phase C18 column (3.9 × 300 mm, PS 5 mm; Waters, MA) at  $\lambda_{\text{max}}$  of 225 nm. A mixture of 70:30 v/v acetonitrile and 0.05 M ammonium acetate buffer (pH 4.5) was used as a mobile phase, running at a flow rate of 2.0 mL/min. The analysis method had been validated. The cumulative amount of drug permeated per unit area ( $\mu\text{g}/\text{cm}^2$ ) was plotted against time (h). The permeation enhancement was assessed with regard to permeation parameters; STZ flux at time 24 h ( $J_{\text{max}}$ ;  $\mu\text{g}/\text{cm}^2/\text{h}$ ), permeability coefficient ( $K_p$ ; cm/h) and enhancement ratio (ER), calculated using the following equations (Al-mahallawi et al., 2014):

$$J_{\text{max}} = \frac{Q}{A \cdot t} \quad (5)$$

$$K_p = \frac{J_{\text{max}}}{C_D} \quad (6)$$

$$ER = \frac{J_{\text{max}} \text{ of mixed micelles formulations}}{J_{\text{max}} \text{ of STZ suspension}} \quad (7)$$

where  $Q$  is the drug amount at 24 h which passes through the corneal barrier ( $\mu\text{g}$ ) to the acceptor chamber,  $A$  is the active area available for permeation (cm<sup>2</sup>),  $t$  is the time of exposure (h), and  $C_D$  is drug concentration loaded into the donor chamber ( $\mu\text{g}/\text{mL}$ ).

After the *ex vivo* permeation experiment, the corneal hydration level was determined. The part of each cornea that was exposed to the dissolution media was rinsed with water to remove any residuals from the formulations, then weighed after removing excess water by filter paper, ( $W_a$ ). Afterwards, it was dried in an oven at 50 °C for 24 h and reweighed ( $W_b$ ). The corneal hydration level (HL) can be calculated using the following equation (Moustafa et al., 2017):

$$\text{HL}\% = \left[ 1 - \frac{W_a}{W_b} \right] \times 100 \quad (8)$$

### Effect of storage on STZ-MMs

Optimized STZ-MMs were kept in stoppered glass vials and stored at (25 °C ± 2) for a period of 6 months. During this storage period, they were evaluated periodically regarding

their  $S_M$ , PS, PDI, and ZP as mentioned previously (Wei et al., 2009).

## In vivo studies

### In vivo corneal tolerance

A histopathological study was done to evaluate the safety of the optimized STZ-MMs to the corneal tissue. Briefly, a 100  $\mu$ L of the optimized STZ-MMs were instilled into the rabbits' right eyes while either saline solution or isopropyl alcohol (100  $\mu$ L) was instilled into the left eyes to act as a negative and positive control, respectively. After 24 h, the rabbits were euthanized (according to the guidelines stated before), and then the corneas were isolated, gently washed with normal saline and then fixed in 10% v/v formalin for 24 h, the tissues were dehydrated with alcohol, placed in melted paraffin beeswax and solidified in block form. Cross-sections (3–4  $\mu$ m) were cut by microtome and stained with hematoxylin and eosin. The stained sections were evaluated using a digital optical microscope (DMS1000 B; Leica, Cambridge, UK) to record any damage caused to the corneas.

### In vivo corneal uptake

Optimized formulations were prepared as previously mentioned after replacing STZ by RhB (0.1% w/w). Each of RhB-loaded MM (100  $\mu$ L) was instilled into the rabbits' right eyes while 0.1% w/w RhB aqueous solution was instilled into the left eyes to act as a reference. After 6 h, the rabbits were euthanized (according to the guidelines stated before), and then the corneas were isolated and rinsed with normal saline. Further, the corneal specimens were directly mounted on glass slides and intracellular fluorescence was observed by confocal laser scanning microscope (LSM 710, Carl Zeiss, Jena, Germany) with an argon laser beam of excitation at 485 nm and emission at 595 nm and the permeation depth was measured at z-axis by LSM software version 4.2 (Carl Zeiss MicroImaging, Jena, Germany) (Salama and Shamma, 2015; Imam et al., 2017).

### Statistical analysis

Design-Expert software (V. 7.0.0, Stat-Ease Inc., Minneapolis, USA) was used for the evaluation of the factorial design. Means were compared by ANOVA-factorial. All measurements were performed in triplicates and the results were expressed as mean values  $\pm$  standard deviation (SD). Using SPSS<sup>®</sup> 19 software (SPSS Inc., Chicago, USA), One-way analysis of variance (ANOVA) followed by Duncan post hoc were applied for multiple group comparisons. The level of significance was set at  $p$ -values  $<$  0.05.

## Results and discussion

### Evaluation of STZ-MMs

In our study, HS15 was mixed with either one of three amphiphiles L121, B58, and F68. These amphiphilic carriers were evaluated for their capacity to form mixed micellar

systems as a potential nanotechnology-based drug delivery system suitable for solubilization and encapsulation of STZ for the treatment of keratomycosis. Two penetration enhancers were used in this study (Trc and PG), both of which thoroughly studied in the transdermal route, but not much evaluated in the ocular route regarding their penetration power and ocular irritation.

### Determination of CMC

The CMC values of the single surfactants were in agreement with the previously determined values in literature where the CMC of HS15, L121, B58, and F68 were 0.009, 0.0056, 0.0063, and 0.02% w/v, respectively (Sezgin et al., 2006; Pepić et al., 2014; Raval et al., 2017). Nevertheless, it should be mentioned that different evaluation procedures of the CMC of these surfactants in aqueous solutions might give slightly different results. The CMC values of the binary mixtures of surfactants were determined and found to be either intermediate between the CMC values of its forming components such as HS15/L121 and HS15/F68 with CMC of 0.0058% w/v and 0.0168% w/v, respectively, or lower than the CMC values of both its forming components such as HS15/B58 with CMC of 0.0039% w/v. These results indicated the ability of the MMs to be formed spontaneously with enhanced solubilization powers, and suggested having an adequate stability (Duan et al., 2015b).

### Analysis of factorial design

A  $3^{1.2^2}$  mixed factorial design was used in this study to evaluate the effects of different variables on the characteristics of the prepared STZ-MMs, as it allows for the investigation of all possible combinations of the levels of the selected variables in each complete trial or replication. Analysis of each response was done individually, and linear regression was used for fitting the data to different order models. Model reduction was adopted when necessary by eliminating insignificant model terms. The final selected model for each response, whether full or reduced was the one with the highest prediction  $R^2$  and the lowest PRESS, it is presented along with its summary statistics in Table 2. In all responses, the difference between the predicted  $R^2$  values and adjusted  $R^2$  was  $\leq$  0.1, which ascertained an adequate fitting of the models to the data, the adequate precision was  $>$  4 which ascertained that used models can evaluate the design space.

### Model analysis of $S_M$

An essential character of MMs is their capability to solubilize poorly-soluble drugs. As shown in Table 1,  $S_M$  of STZ-MMs ranged from  $2.02 \pm 0.10$  mg/mL to  $7.79 \pm 0.17$  mg/mL. All prepared MMs led to sharp increase in STZ solubility according to the calculated  $F_s$ , ranging from 86-fold to 338-fold compared to STZ aqueous solubility (0.023 mg/mL). ANOVA-factorial showed that both A: type of auxiliary surfactant and C: total surfactants: drug ratio had significant effects on  $S_M$  (Table 2). As for the effect of type of auxiliary surfactant on

$S_M$ . Duncan post hoc test showed that MMs prepared using B58 (B58-MMs) had the highest  $S_M$  compared to those prepared using L121 (L121-MMs) then those prepared with F68 (F68-MMs), the differences between the three types were significant (B58 > L121 > F68) (Figure 1(I-A<sub>i</sub>)). This low ability of F68-MMs to solubilize STZ could be attributed to the high

hydrophilicity of F68, expressed by the large number of polyethylene oxide PEO units present in its structure (PEO = 152) compared to the low number of PEO in both L121 (PEO = 10) and B58 (PEO = 20) (Panda and Kamil, 2017), these PEO units formed a highly dense hydrophilic corona, that acted as a shield against the penetration of hydrophobic STZ into the core (Turco Liveri et al., 2012). Furthermore, it is well known that the stronger the hydrophobic interactions between the hydrophobic segments of mixed surfactants, the lower the CMC of their resulted mixture (Li et al., 2011). These hydrophobic interactions are responsible of maintaining the shell integrity of MMs and preventing their dissociation into monomers. Since, the mixture of HS15/B58 had the lowest CMC values as previously determined, it was assumed to have the strongest hydrophobic interactions. This assumption was supported by the results of the calculated stability index (SI), which showed that B58-MMs had the highest SI values (0.65, 0.68, 0.97, and 0.95) followed by L121-MMs (0.32, 0.31, 0.65, and 0.58), then F68-MMs (0.25, 0.25, 0.42, and 0.43). This meant that after the passage of 48 h, only B58-MMs were able to keep their assembled structure and so preserved STZ solubilized within its core, while L121-MMs and F68-MMs were unable to maintain their shell integrity and caused STZ precipitation.

Results also showed that increasing the total surfactant to drug ratio significantly enhanced  $S_M$  of STZ (Figure 1(I-A<sub>ii</sub>)).

**Table 2.** Significance of different model terms appearing in the final model for each response, together with models evaluation.

Component	p-Value			
	$S_M$ (mg/mL)	PS (nm)	PDI	ZP (mV)
A	<b>&lt;0.0001</b>	<b>&lt;0.0001</b>	<b>0.0062</b>	<b>&lt;0.0001</b>
B	–	0.1209	–	<b>0.0041</b>
C	<b>&lt;0.0001</b>	<b>&lt;0.0001</b>	<b>&lt;0.0001</b>	0.0709
AB	–	–	–	<b>0.0056</b>
AC	<b>0.0119</b>	<b>0.021</b>	–	<b>&lt;0.0001</b>
BC	–	–	–	<b>&lt;0.0001</b>
ABC	–	–	0.0597	–
RMSE	0.33	0.73	0.03	2.15
R <sup>2</sup>	0.9782	0.9683	0.8322	0.9448
Adjusted R <sup>2</sup>	0.9722	0.9572	0.7855	0.9094
Prediction R <sup>2</sup>	0.9613	0.9369	0.7016	0.8379
PRESS	3.48	18.21	0.029	190.04
Adeq Precision	34.505	28.293	12.64	15.189

A: Auxiliary surfactant type; B: Penetration enhancer type; C: Total surfactants: drug ratio;  $S_M$ : solubility of STZ in MMs; PS: particle size; PDI: polydispersity index; ZP: zeta potential; RMSE: Root mean square error; R<sup>2</sup>: Regression coefficient.

<sup>a</sup> p Values for significant terms are shown in bold face.

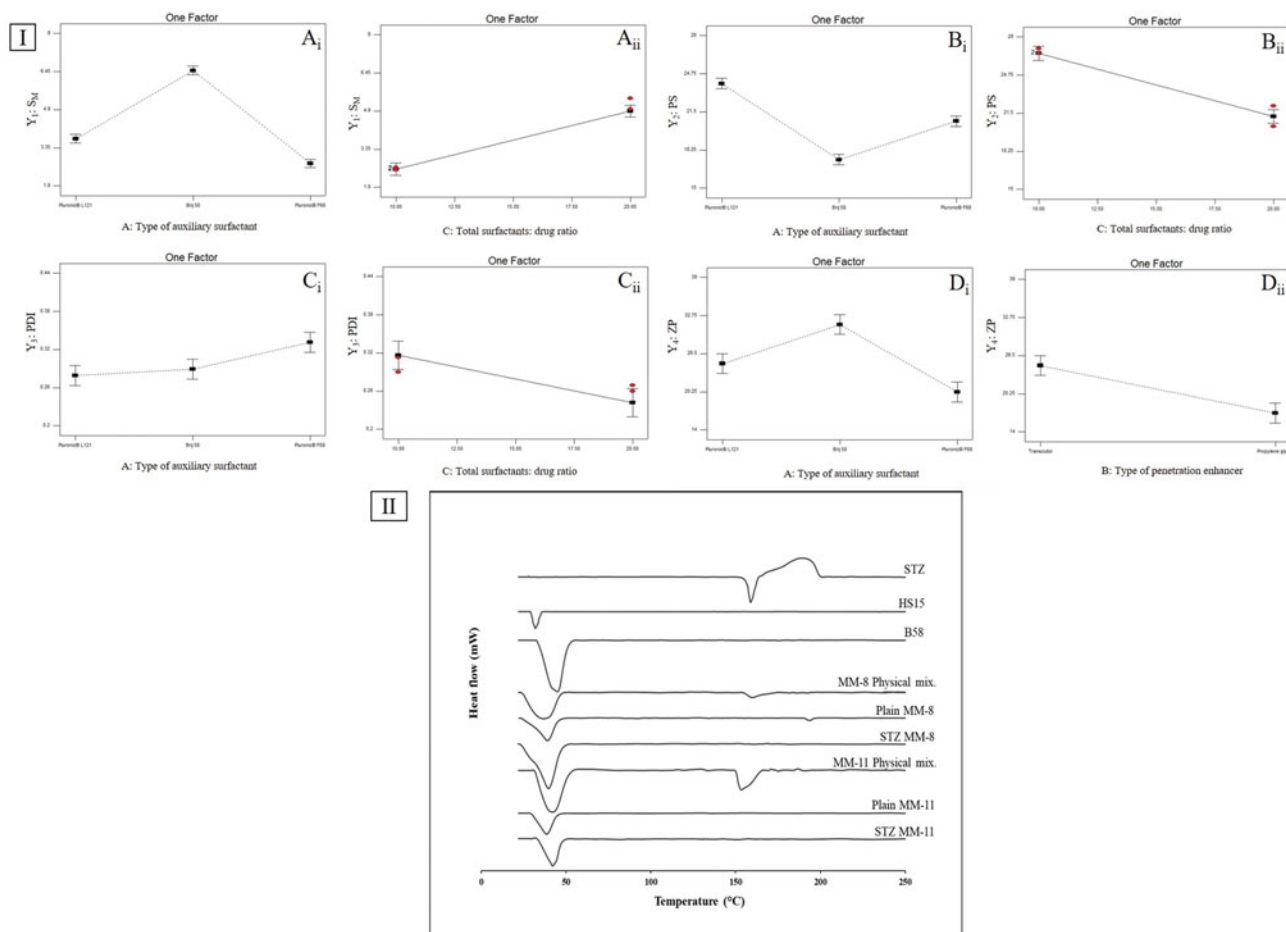


**Figure 1.** (I) line plots of the significant effects of type of auxiliary surfactant, total surfactants: drug ratio and type of penetration enhancer on (A)  $S_M$ , (B) PS, (C) PDI, and (D) ZP. (II) DSC thermograms of STZ, HS15, B58, MM-8 physical mix, plain MM-8, STZ-MM-8, MM-11 physical mix, plain MM-11, and STZ-MM-11.

The higher the amount of total surfactants existed in the system, the larger the number of MMs assembled, and so the greater the enhancement in the solubilization of STZ (Pepić et al., 2014). On the contrary, increasing the amount of drug relative to the total surfactants might have led to rapid saturation of the inner cores of the MMs, causing the precipitation of excess drug (Fares et al., 2018).

### Model analysis of PS

PS of the prepared MMs, is a crucial aspect in determining their suitability for ocular administration, as it affects their ocular tolerance and their disposition following topical administration (Amrite and Kompella, 2005). As shown in Table 1, PS of STZ-MMs ranged from  $15.87 \pm 0.71$  nm to  $26.87 \pm 1.05$  nm. All prepared MMs were in the nanometric scale ( $<30$  nm), thus they are anticipated to have good corneal permeability, prolonged residence time in the ocular circulation, and good ocular tolerance with low chance of discomfort (Bhatta et al., 2012). ANOVA-factorial showed that both A: type of auxiliary surfactant and C: total surfactants: drug ratio had significant effects on PS (Table 2).

As for the effect of type of auxiliary surfactant on PS, Duncan post hoc test showed that B58-MMs had the lowest PS compared to F68-MMs then L121-MMs, the differences between the three types were significant ( $B58 < F68 < L121$ ) (Figure 1(I-B<sub>ij</sub>)). This very low size of B58-MMs might be attributed to the previously mentioned strong hydrophobic interactions with HS15, which lead to formation of compact spherical micelles with small size. On the contrary, both L121 and F68 had weaker interactions with HS15 which was assumed to cause loosening and elongation of the formed MMs (Vautier-Giongo et al., 2005).

Results also showed that increasing the total surfactant to drug ratio significantly decreased PS of MMs (Figure 1(I-B<sub>ij</sub>)). Where increasing the total surfactant to drug ratio led to the formation of a large number of MMs that was able to incorporate STZ within their core without extensive core swelling. In contrast, decreasing the total surfactant to drug ratio pressurized the solubilization of STZ into the core of a limited number of MMs, which caused swelling of the hydrophobic core region and so enlargement of PS (Fares et al., 2018).

### Model analysis of PDI

PDI indicates the width of the PS distribution. PDI values closer to 0 denotes a highly homogenous PS distribution, in contrast, PDI values closer to unity denotes a highly poly-

dispersed PS distribution (Das et al., 2012). PDI of STZ-MMs ranged from  $0.217 \pm 0.01$  to  $0.415 \pm 0.03$ . All measured formulations were with an adequate homogenous particle distribution. ANOVA-factorial showed that both A: type of auxiliary surfactant and C: total surfactants: drug ratio had significant effects on PDI (Table 2).

As for the effect of type of auxiliary surfactant on PDI, Duncan post hoc test showed that F68-MMs had the highest PDI compared to B58-MMs and L121-MMs, the difference was significant for F68 only ( $F68 > B58 = L121$ ) (Figure 1(I-C<sub>ij</sub>)), this can be attributed to the variation in their molecular weights (Mwts). F68 has the highest Mwt (8400), so mixing it with HS15 increased the average Mwt of total surfactant mixture, this might cause a less kinetically restricted encapsulation of the drug which increased the PDI due to low uniformity of PS distribution (Nour et al., 2016).

Increasing total surfactant to drug ratio led to a significant decrease in the PDI (Figure 1(I-C<sub>ij</sub>)), which might be attributed to the increased solubilization of STZ within the core of the formed MMs, causing less amount of free drug available to form aggregates.

### Model analysis of ZP

ZP is a measure of the net charge attained by the surface of dispersed MMs. The magnitude of ZP gives a good indication on the physical stability of the MMs, ZP value of more than  $\pm 15$  mV indicates a stable system (Rajagopalan and Hiemenz, 1997). On the other hand, the sign of ZP gives indication on the nature of possible interaction with the target tissues. As shown in Table 3, ZP of STZ-MMs ranged from  $15.85 \pm 1.77$  mV to  $36.89 \pm 2.81$  mV. All formulations had positive charge with values  $>15$  mV, due to the presence of cationic nitrogen atoms in the structure of STZ, which imparted a positive charge dominating over the neutral charge of the used nonionic surfactants (Qushawy et al., 2018). These values are high enough to prevent aggregation due to the electrostatic repulsion between the micelles, this is in addition to the steric stabilization imparted by the surfactants used. Moreover, the positive charge of the MMs is favorable for the ocular route, as it increases electrostatic interactions with the negatively charged mucin, which enhances corneal adhesion and retention (Yoncheva et al., 2011). ANOVA-factorial showed that both A: type of auxiliary surfactant and B: type of penetration enhancer on ZP (Table 2).

As for the effect of type of auxiliary surfactant on ZP, Duncan post hoc test showed that B58-MMs had the highest ZP compared to those prepared using F68-MMs and L121-

**Table 3.** Predicted values of different responses for optimized formulations (MM-8 and MM-11) compared to the actual values together with the prediction intervals and percent deviations.

Formula	Validity parameters	Y <sub>1</sub> : S <sub>M</sub> (mg/mL)	Y <sub>2</sub> : PS (nm)	Y <sub>3</sub> : PDI	Y <sub>4</sub> : ZP (mV)
MM-8	Predicted value	7.69	15.88	0.247	29.38
	95% prediction interval	6.92–8.46	14.12–17.64	0.18–0.32	23.89–34.86
	Actual values	7.79	15.87	0.249	28.95
	% Deviation	1.29	0.08	0.81	1.45
MM-11	Predicted value	7.69	16.37	0.230	22.90
	95% prediction interval	6.92–8.46	14.61–18.13	0.16–0.3	17.41–28.38
	Actual values	7.59	16.39	0.234	23.33
	% Deviation	1.31	0.11	1.87	1.89

SM: solubility of STZ in MMs; PS: particle size; PDI: polydispersity index; ZP: zeta potential.

MMs, the difference was significant for B58 only (B58 > F68 = L121) (Figure 1(I-D<sub>i</sub>)), which might be attributed to the increased solubilization of STZ, causing further protonation of the present cationic nitrogen atoms, increasing the positive charge of the formed MMs. Results also showed that changing type of penetration enhancer from Trc to PG significantly decreased the ZP (Figure 1(I-D<sub>ii</sub>)).

### Testing the validity of the suggested models and selection of optimized STZ-MMs

After comparing the actual and the predicted values for all twelve suggested design points using % deviation, average % deviation was found to be <2% for all responses, also all measured mean values of the responses fell within the corresponding 95% PI. This proved that the final selected models were capable of representing and predicting the studied responses within data uncertainty. Based on the DF approach, a number of solutions representing different combinations of factors levels were suggested, as they establish the predetermined constraints. Two combinations of which were selected, as they had the highest desirability, A: B58, B: Trc, C: 20:1 (**0.891**), and A: B58, B: PG, C: 20:1 (**0.866**). These combinations had already been prepared as design points under the name MM-8 and MM-11, respectively. Table 3 shows the predicted and actual values for all responses of both optimized formulations (MM-8 and MM-11) together with their 95% PIs and calculated % deviation.

### Differential scanning calorimetry (DSC)

In Figure 1(II), The DSC scan of STZ, HS15 and B58 showed melting peaks at 156.6, 30, and 39.38 °C, respectively, which matched their intrinsic melting points (Aggarwal and Jindal, 2014; Liu et al., 2016). The endothermic peak of STZ was preserved in the physical mixtures, while it was absent in the thermograms of plain and STZ-MMs (MM-8 and MM-11), this

might suggest the transformation of STZ from crystalline to molecular form due to the inclusion and complete dispersion of STZ in the nano-micellar system during preparation (Fouad et al., 2017). The thermograms of the physical mixtures, lyophilized plain and STZ-loaded optimized formulations (MM-8 and MM-11) revealed a broad peak ranging from 25 to 50 °C representing the peaks of HS15 and B58 fused.

### Transmission electron microscopy (TEM)

TEM imaging helped in evaluating the morphology of the optimized formulations, as well as in assessing the PS values obtained from the Zetasizer analyzer (Abd-Elsalam et al., 2018). Figure 3(I) revealed that both (MM-8 and MM-11) were spherical in shape with narrow size distribution and no signs of large aggregates, which might be attributed to the previously mentioned electrostatic and steric barriers between the formed MMs. Also, the mean PS observed in the TEM micrographs was in a good harmony with that obtained previously from the Zetasizer analyzer which was less than 30 nm.

### Mucoadhesion studies

The evaluation of mucoadhesive properties of the optimized formulations (MM-8 and MM-11) was necessary to investigate their corneal retention behavior, which is a crucial factor that can limit their ocular bioavailability. PS, ZP, and Turbidity values of Mucin, MM-8, and MM-11 aqueous dispersions were used as a reference. In both Mucin mixed formulations (MM-8/mucin and MM-11/mucin), PS has undergone a gradual increase till the end of the incubation period (Figure 2(I-A)), while for the ZP, their positive charge was reduced to the extent it attained a negative charge after only 6 h and continued to drop till approximately reaching the same negative charge as pure mucin (Figure 2(I-B)). The turbidity of mucin

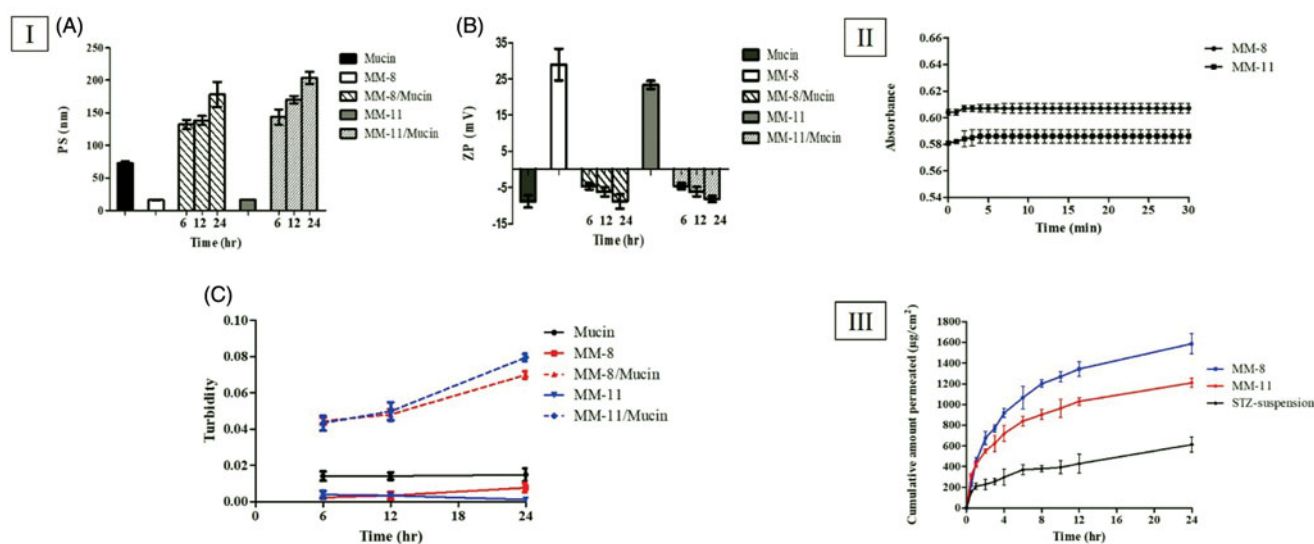


**Figure 2.** (I) Mucoadhesion results: (A) PS measurements, (B) ZP measurements and (C) Turbidimetric measurements. (II) Evolution of the absorbance of optimized formulations (MM-8 and MM-11) after 100-folds dilution in STF. (III) The ex-vivo permeation profile of STZ from optimized formulations (MM-8 and MM-11) compared to the STZ-suspension.

mixed formulations was increased over the time and was found to be higher than native mucin, while that of mucin, MM-8 and MM-11 aqueous dispersions was found to be nearly constant throughout the incubation period (Figure 2(I-C)). This proves that the change in the turbidity of MMs/mucin dispersions wasn't caused by the motion of particles. The increase in PS, decrease in ZP and increase in turbidity of (MM-8/mucin and MM-11/Mucin) could be attributed to the electrostatic interaction of positively charged surface layer of these formulations with negatively charged sialic groups of mucin as previously explained by several studies (Bhatta et al., 2012), which can lead to an anticipated increase in the retention time to the mucosal surface.

### Stability upon dilution

In order to ascertain the capability of the optimized formulations (MM-8 and MM-11) to withstand dilution with lacrimal fluid without drug precipitation after being administered to the eye. The formulations were diluted 100-fold and the absorbances were recorded immediately and monitored for 30 min. The first few minutes demonstrated an initial rise in absorbance, followed by a complete and stable recovery, as shown in Figure 2(II). This result indicated the ability of the optimized formulations to restore the micelle-medium partition equilibrium upon initial dilution, which can be attributed to the extremely low CMC of the formed MMs, which imparted high physical stability and preserved STZ encapsulation (Alvarez-Rivera et al., 2016).

### Ex vivo corneal permeation

The drug permeation from the STZ-suspension, MM-8, and MM-11 formulations was measured at certain time intervals as shown in Figure 2(III). On comparing the corneal permeability parameters, both formulations (MM-8 and MM-11) significantly increased the flux after 24 h ( $p < 0.05$ ), where the  $J_{max}$  values of MM-8 ( $66.12 \pm 4.09 \mu\text{g}/\text{cm}^2/\text{h}$ ) and MM-11 ( $50.38 \pm 1.80 \mu\text{g}/\text{cm}^2/\text{h}$ ) were 2.59 and 1.97 times greater than that of STZ-suspension ( $25.55 \pm 3.14 \mu\text{g}/\text{cm}^2/\text{h}$ ), respectively, as calculated by the ER. Both formulations also resulted in a significantly higher permeability coefficient ( $K_p$ ) compared to that of STZ-suspension ( $p < 0.05$ ), where  $K_p$  of MM-8, MM-11 and STZ-suspension were  $132.2 \pm 8.18 \times 10^{-4} \text{cm}/\text{h}$ ,  $100.7 \pm 3.6 \times 10^{-4} \text{cm}/\text{h}$ , and  $51.1 \pm 6.28 \times 10^{-4} \text{cm}/\text{h}$ , respectively. This can be attributed to various reasons: (1) the significant increase in the solubility of STZ ( $>7.5 \text{mg}/\text{mL}$ ) which enhanced its concentration in the precorneal tear film (Malhotra and Majumdar, 2001), (2) the nanometric size of the formulations ( $<20 \text{nm}$ ) which facilitated their passage through the hydrated network of the corneal stroma (Zhou et al., 2017), (3) the mucoadhesive nature due electrostatic adsorption of positively STZ-MMs to the corneal surface which enhanced the precorneal residence time (Ban et al., 2017), and (4) the composition of the MMs including non-ionic surfactants (HS15 and B58) and penetration enhancers (Trc and PG) which increased the mucosal membrane permeability, by loosening the tight junctions of the corneal

**Table 4.** Effect of storage on the physicochemical properties of optimized STZ-MMs formulations (MM-8 and MM-11).

Formula	Storage period	$S_M$ (mg/mL)	PS (nm)	PDI	ZP (mV)
MM-8	Fresh	$7.79 \pm 0.17$	$15.87 \pm 0.71$	$0.249 \pm 0.04$	$28.95 \pm 4.38$
	1 Month	$7.72 \pm 0.28$	$15.99 \pm 0.17$	$0.250 \pm 0.01$	$28.12 \pm 2.93$
	2 Months	$7.69 \pm 0.15$	$16.02 \pm 0.01$	$0.249 \pm 0.05$	$28.80 \pm 1.99$
	3 Months	$7.64 \pm 0.25$	$16.02 \pm 0.33$	$0.247 \pm 0.02$	$25.10 \pm 4.10$
	6 Months	$7.61 \pm 0.37$	$16.04 \pm 0.23$	$0.249 \pm 0.04$	$25.21 \pm 0.76$
MM-11	Fresh	$7.59 \pm 0.16$	$16.39 \pm 0.04$	$0.234 \pm 0.04$	$23.33 \pm 1.17$
	1 Month	$7.53 \pm 0.08$	$16.38 \pm 0.08$	$0.239 \pm 0.07$	$25.20 \pm 1.85$
	2 Months	$7.56 \pm 0.14$	$16.47 \pm 0.45$	$0.242 \pm 0.03$	$25.00 \pm 2.83$
	3 Months	$7.51 \pm 0.12$	$16.52 \pm 0.33$	$0.247 \pm 0.06$	$26.20 \pm 4.53$
	6 Months	$7.25 \pm 0.31$	$16.83 \pm 0.39$	$0.271 \pm 0.04$	$25.70 \pm 0.42$

$S_M$ : solubility of STZ in MMs; PS: particle size; PDI: polydispersity index; ZP: zeta potential.

epithelial barriers, allowing the penetration of STZ via the paracellular route (Malhotra and Majumdar, 2001). It was also noticed that optimized formulation MM-8 formulated with Trc showed higher  $J_{max}$  and  $K_p$  than MM-11 formulated with PG, this might be due to the more effective interaction of Trc with the corneal membrane lipids, causing an increased membrane fluidity and permeability (Caddeo et al., 2013).

Corneal hydration levels (HL) were calculated to evaluate the damage of the corneal tissues following the *ex vivo* study. Normal cornea has a hydration level up to 76–80%, while a hydration level of 83–92% denotes damage of the corneal epithelial and/or endothelial layers (Li et al., 2013; El-Salamouni et al., 2018). In this study, HL of the excised corneas exposed to MM-8, MM-11 and STZ-suspension were  $78.13 \pm 0.41\%$ ,  $78.62 \pm 0.73\%$ , and  $79.03 \pm 0.57\%$ , respectively. Each was within the normal range, which implied the integrity of the corneal tissues throughout the experiments.

### Effect of storage

After the completion of the storage period, there was no evidence of precipitation or any alteration in appearance in both of (MM-8 and MM-11) at  $25 \pm 2^\circ\text{C}$  for 6 months. In Table 4, the parameters of the stored formulations ( $S_M$ , PS, PDI, and ZP) were measured and showed no significant difference ( $p > 0.05$ ) when compared to that of the fresh ones using One-way ANOVA. These results indicated the high structural stability of the optimized MMs, and ascertained the previously obtained results.

### In vivo studies

#### In vivo corneal tolerance

Histopathological evaluation is necessary to evaluate the biocompatibility of the utilized surfactants and penetration enhancers (Trc and PG) on the corneal tissues. The safety of optimized formulations (MM-8 and MM-11) was examined in comparison to isopropyl alcohol (positive control) and normal saline solution (negative control). As represented in Figure 3(II-A), corneal tissues treated with normal saline solution showed normal histological structures of the epithelial, the underlying stroma and the endothelial layers. On the other hand, corneal tissues exposed to isopropyl alcohol (Figure 3(II-B)) showed disfiguration and desquamation of the lining epithelium layer. Applying the optimized

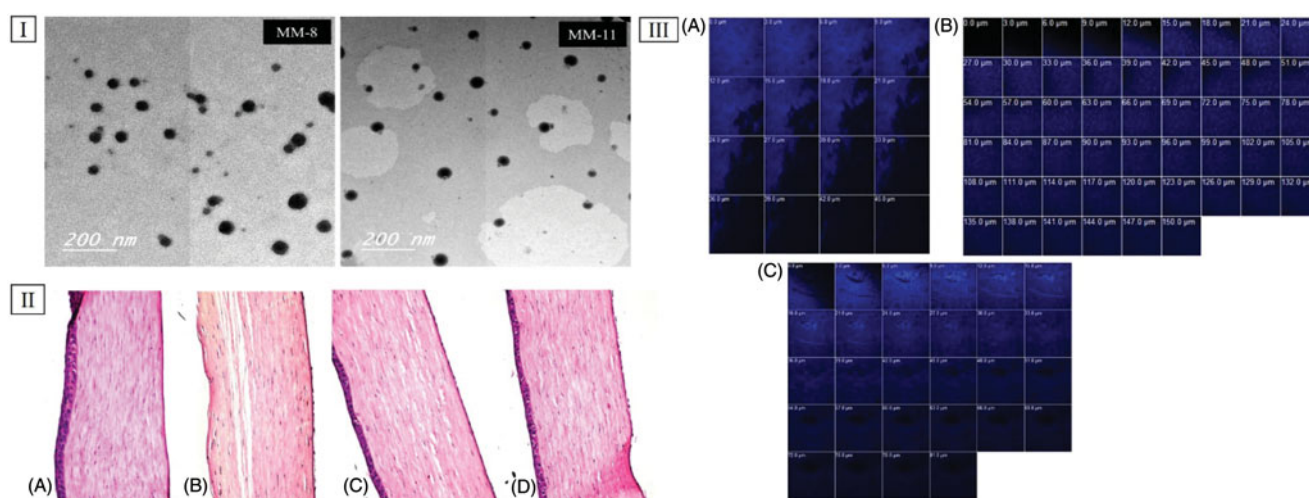


**Figure 3.** (I) Transmission electron micrographs of optimized formulations (MM-8 and MM-11). (II) Photomicrographs of the rabbits' corneas after instillation of; (A) normal saline solution (negative control), (B) Isopropyl alcohol (positive control), (C) MM-8 formulation and (D) MM-11 formulation. (III) Confocal laser scanning micrographs of the rabbits' corneas after instillation of (A) 0.1% RhB aqueous solution, (B) RhB loaded MM-8, and (C) RhB loaded MM-11.

formulations (MM-8 and MM-11) to corneal tissues (Figure 3(II-C and D)) showed no sign of inflammation in the same manner as found with normal saline solution. These results ascertained the nonirritant nature of the optimized formulations and the capability of using them for ocular applications (Ameeduzzafar et al., 2018), which was in agreement with the studies that confirmed the safety of incorporating Trc (ElKasabgy, 2014) and PG (Kesavan et al., 2013) in the ocular preparations at ratios even higher than that used in our study.

### In vivo corneal uptake

To evaluate the capacity of the optimized formulations (MM-8 and MM-11) and to improve the corneal permeation of STZ, CLSM was utilized to observe the transcorneal behavior of RhB labeled formulations after instillation, by tracking fluorescence signals inside the corneal tissues. As shown in Figure 3(III), RhB solution was detected at a depth of 45 μm, while RhB-MM-8 and RhB-MM-11 were detected at a depth of 150 and 81 μm, respectively. It was clear that MM-8 improved the penetration depth of RhB by 3.3-fold, compared to MM-11 which improved the penetration depth of RhB by 1.8-fold only. This confirmed that RhB-MM-8 exhibited deeper penetration ability into cornea than RhB-MM-11 or RhB solution, which was in agreement with the *ex vivo* permeation results with the same order of permeation enhancement (MM-8 > MM-11 > STZ-suspension). These results confirmed the corneal permeability enhancement achieved by the prepared HS15 based binary mixed micellar system to STZ.

### Conclusion

This study investigated the use of STZ as a promising ocular treatment for keratomycosis. STZ-MMs were successfully prepared using thin-film hydration method based on a  $3^{1.2^2}$  mixed factorial design. STZ-MMs succeeded in enhancing solubility of STZ up to 338.82-fold. Two optimized

formulations (MM-8 and MM-11) were selected for further investigations to prove their suitability for ocular delivery. From which, the optimized formulation (MM-8) showed superiority in the *ex vivo* and *in vivo* permeation studies when compared to the STZ-Suspension. Accordingly, MM-8 could be considered a promising ocular delivery carrier with high physical stability, good biocompatibility and enhanced corneal permeation and retention.

### Disclosure statement

The authors report no conflicts of interest.

### ORCID

Nihal Farid Younes  <http://orcid.org/0000-0002-5105-3669>

### References

- Abd-El Salam WH, El-Zahaby SA, Al-Mahallawi AM. (2018). Formulation and in vivo assessment of terconazole-loaded polymeric mixed micelles enriched with Cremophor EL as dual functioning mediator for augmenting physical stability and skin delivery. *Drug Deliv* 25:484–92.
- Abdelbary GA, Tadros MI. (2013). Brain targeting of olanzapine via intranasal delivery of core-shell difunctional block copolymer mixed nanomicellar carriers: in vitro characterization, ex vivo estimation of nasal toxicity and in vivo biodistribution studies. *Int J Pharm* 452:300–10.
- Aggarwal AK, Jindal P. (2014). Modification of crystallization behaviour of sertaconazole by preparing its solid dispersions. *J Pharm Allied Health Sci* 4:1.
- Al-Badriyeh D, Neoh CF, Stewart K, Kong DC. (2010). Clinical utility of voriconazole eye drops in ophthalmic fungal keratitis. *Clin Ophthalmol* 4:391.
- Al-mahallawi AM, Khowessah OM, Shoukri RA. (2014). Nano-transfersomal ciprofloxacin loaded vesicles for non-invasive trans-tympanic otological delivery: in-vitro optimization, ex-vivo permeation studies, and in-vivo assessment. *Int J Pharm* 472:304–14.
- Alani AW, Rao DA, Seidel R, et al. (2010). The effect of novel surfactants and solutol<sup>®</sup> HS 15 on paclitaxel aqueous solubility and permeability across a Caco-2 monolayer. *J Pharm Sci* 99:3473–85.

- Albet C, Fernández J, Sacristán A, Ortiz J. (1992). Physico-chemical properties, analytical determinations and stability of sertaconazole nitrate. *Arzneimittelforschung* 42:695–8.
- Aliabadi HM, Lavasanifar A. (2006). Polymeric micelles for drug delivery. *Expert Opin Drug Deliv* 3:139–62.
- Alvarez-Rivera F, Fernández-Villanueva D, Concheiro A, Alvarez-Lorenzo C. (2016).  $\alpha$ -Lipoic acid in soluplus® polymeric nanomicelles for ocular treatment of diabetes-associated corneal diseases. *J Pharm Sci* 105:2855–63.
- Ameeduzzafar, Imam SS, Bukhari SNA, et al. (2018). Preparation and evaluation of novel chitosan: gelrite ocular system containing besifloxacin for topical treatment of bacterial conjunctivitis: scintigraphy, ocular irritation and retention assessment. *Artif Cells Nanomed Biotechnol* 46:959–67.
- Amrite AC, Kompella UB. (2005). Size-dependent disposition of nanoparticles and microparticles following subconjunctival administration. *J Pharm Pharmacol* 57:1555–63.
- Ansari Z, Miller D, Galor A. (2013). Current thoughts in fungal keratitis: diagnosis and treatment. *Curr Fungal Infect Rep* 7:209–18.
- Ban J, Zhang Y, Huang X, et al. (2017). Corneal permeation properties of a charged lipid nanoparticle carrier containing dexamethasone. *Int J Nanomedicine* 12:1329.
- Bhatta R, Chandasana H, Chhonker Y, et al. (2012). Mucoadhesive nanoparticles for prolonged ocular delivery of natamycin: in vitro and pharmacokinetics studies. *Int J Pharm* 432:105–12.
- Caddeo C, Sales OD, Valenti D, et al. (2013). Inhibition of skin inflammation in mice by diclofenac in vesicular carriers: liposomes, ethosomes and PEVs. *Int J Pharm* 443:128–36.
- Chen L, Sha X, Jiang X, et al. (2013). Pluronic P105/F127 mixed micelles for the delivery of docetaxel against Taxol-resistant non-small cell lung cancer: optimization and in vitro, in vivo evaluation. *Int J Nanomedicine* 8:73.
- Chetoni P, Buralassi S, Monti D, Saettone M. (2003). Ocular toxicity of some corneal penetration enhancers evaluated by electrophysiology measurements on isolated rabbit corneas. *Toxicol In Vitro* 17:497–504.
- Croxtall JD, Plosker GL. (2009). Sertaconazole. *Drugs* 69:339–59.
- Das S, Ng WK, Tan RB. (2012). Are nanostructured lipid carriers (NLCs) better than solid lipid nanoparticles (SLNs): development, characterizations and comparative evaluations of clotrimazole-loaded SLNs and NLCs? *Eur J Pharm Sci* 47:139–51.
- Di Prima G, Saladino S, Bongiovì F, et al. 2017. Novel Inulin-Based Mucoadhesive Micelles Loaded With Corticosteroids as Potential Transcorneal Permeation Enhancers. *Eur J Pharm Biopharm* 117:385–399.
- Duan Y, Cai X, Du H, Zhai G. (2015). Novel in situ gel systems based on P123/TPGS mixed micelles and gellan gum for ophthalmic delivery of curcumin. *Colloids Surf B Biointerfaces* 128:322–30.
- Duan Y, Wang J, Yang X, et al. (2015). Curcumin-loaded mixed micelles: preparation, optimization, physicochemical properties and cytotoxicity in vitro. *Drug Deliv* 22:50–7.
- El-Salamouni NS, Farid RM, El-Kamel AH, El-Gamal SS. (2018). Nanostructured lipid carriers for intraocular brimonidine localization; development, in-vitro and in-vivo evaluation. *J Microencapsul* 35:102–113.
- ElKasabgy NA. (2014). Ocular supersaturated self-nanoemulsifying drug delivery systems (S-SNEDDS) to enhance econazole nitrate bioavailability. *Int J Pharm* 460:33–44.
- Fares AR, ElMeshad AN, Kassem MA. (2018). Enhancement of dissolution and oral bioavailability of lacidipine via pluronic P123/F127 mixed polymeric micelles: formulation, optimization using central composite design and in vivo bioavailability study. *Drug Deliv* 25:132–42.
- Fernández-Ferreiro A, Gonzalez-Barcia M, Gil-Martínez M, et al. others, (2016). Current use of antifungal eye drops and how to improve therapeutic aspects in keratomycosis. *Fungal Genom Biol* 6:2.
- Fouad SS, Habib BA, Elsayed GM. (2017). Tri-block co-polymer nanocarriers for enhancement of oral delivery of felodipine: preparation, in-vitro characterization and ex-vivo permeation. *J Liposome Res* 28:182–192.
- Gan L, Gan Y, Zhu C, et al. (2009). Novel microemulsion in situ electrolyte-triggered gelling system for ophthalmic delivery of lipophilic cyclosporine A: in vitro and in vivo results. *Int J Pharm* 365:143–9.
- Grimaudo MA, Pescina S, Padula C, et al. (2018). Poloxamer 407/TPGS mixed micelles as promising carriers for cyclosporine ocular delivery. *Mol Pharm* 15:571–84.
- Habib BA, AbouGhaly MH. (2016). Combined mixture-process variable approach: a suitable statistical tool for nanovesicular systems optimization. *Expert Opin Drug Deliv* 13:777–88.
- He D, Hao J, Gao S, et al. (2016). Etiological analysis of fungal keratitis and rapid identification of predominant fungal pathogens. *Mycopathologia* 181:75–82.
- Hou J, Sun E, Sun C, et al. (2016). Improved oral bioavailability and anticancer efficacy on breast cancer of paclitaxel via Novel Soluplus®—Solutol® HS15 binary mixed micelles system. *Int J Pharm* 512:186–193.
- Higa LH, Schilrreff P, Perez AP, et al. (2013). The intervention of nanotechnology against epithelial fungal diseases. *J Biomater Tissue Eng* 3:70–88.
- Huang Y-B, Tsai Y-H, Yang W-C, et al. (2004). Once-daily propranolol extended-release tablet dosage form: formulation design and in vitro/in vivo investigation. *Eur J Pharm Biopharm* 58:607–14.
- Imam SS, Bukhari SNA, Ahmed J, Ali A, et al. (2017). Formulation and optimization of Levofloxacin loaded Chitosan Nanoparticle for Ocular delivery: in-vitro characterization, ocular tolerance and antibacterial activity. *Int J Biol Macromol* 108:650–59.
- Jaiswal M, Kumar M, Pathak K. (2015). Zero order delivery of itraconazole via polymeric micelles incorporated in situ ocular gel for the management of fungal keratitis. *Colloids Surf B Biointerfaces* 130:23–30.
- Kaur IP, Rana C, Singh H. (2008). Development of effective ocular preparations of antifungal agents. *J Ocul Pharmacol Ther* 24:481–94.
- Kaur IP, Smitha R. (2002). Penetration enhancers and ocular bioadhesives: two new avenues for ophthalmic drug delivery. *Drug Dev Ind Pharm* 28:353–69.
- Kesavan K, Kant S, Singh PN, Pandit JK. (2013). Mucoadhesive chitosan-coated cationic microemulsion of dexamethasone for ocular delivery: in vitro and in vivo evaluation. *Curr Eye Res* 38:342–52.
- Li J, Wu L, Wu W, et al. (2013). A potential carrier based on liquid crystal nanoparticles for ophthalmic delivery of pilocarpine nitrate. *Int J Pharm* 455:75–84.
- Li X, Zhang Y, Fan Y, et al. (2011). Preparation and evaluation of novel mixed micelles as nanocarriers for intravenous delivery of propofol. *Nanoscale Res Lett* 6:275.
- Liu L, Mao K, Wang W, et al. (2016). Kolliphor® HS 15 micelles for the delivery of coenzyme Q10: preparation, characterization, and stability. *AAPS PharmSciTech* 17:757–66.
- Lu Y, Park K. (2013). Polymeric micelles and alternative nanonized delivery vehicles for poorly soluble drugs. *Int J Pharm* 453:198–214.
- Mahaling B, Katti DS. (2016). Understanding the influence of surface properties of nanoparticles and penetration enhancers for improving bioavailability in eye tissues in vivo. *Int J Pharm* 501:1–9.
- Malhotra M, Majumdar D. 2001. Permeation through cornea. *Indian J Exp Biol* 39:11–24.
- Mandal A, Bisht R, Rupenthal ID, Mitra AK. 2017. Polymeric micelles for ocular drug delivery: From structural frameworks to recent preclinical studies. *J Control Release* 248:96–116.
- Mehta P, Al-Kinani AA, Arshad MS, et al. (2017). Development and characterisation of electrospun timolol maleate-loaded polymeric contact lens coatings containing various permeation enhancers. *Int J Pharm* 532:408–20.
- Moustafa MA, Elnaggar YS, El-Refaie WM, Abdallah OY. (2017). Hyalugel-integrated liposomes as a novel ocular nanosized delivery system of fluconazole with promising prolonged effect. *Int J Pharm* 534:14–24.
- Nettey H, Darko Y, Bamiro OA, Addo RT. 2016. Ocular barriers. In: Addo RT, ed. *Ocular drug delivery: advances, challenges and applications*. Cham, Switzerland: Springer, 27–36.
- Nour SA, Abdelmalak NS, Naguib MJ, et al. (2016). Intranasal brain-targeted clonazepam polymeric micelles for immediate control of

- status epilepticus: in vitro optimization, ex vivo determination of cytotoxicity, in vivo biodistribution and pharmacodynamics studies. *Drug Deliv* 23:3681–95.
- Panda M, Kamil M. 2017. Interaction of oxy-diester-linked cationic gemini surfactants with nonionic amphiphiles in aqueous medium. *Colloid Polym Sci* 295:2363–71.
- Park SH, Park JO. 1998. Simultaneous optimization of multiple responses using a weighted desirability function. In: Abraham B, ed. *Quality Improvement through Statistical Methods*. Boston, MA: Birkhäuser, 299–311.
- Pepić I, Lovrić J, Hafner A, Filipović-Grčić J. (2014). Powder form and stability of Pluronic mixed micelle dispersions for drug delivery applications. *Drug Dev Ind Pharm* 40:944–51.
- Prajna NV, Srinivasan M, Lalitha P, et al. others, (2013). Differences in clinical outcomes in keratitis due to fungus and bacteria. *JAMA Ophthalmol* 131:1088–9.
- Qushawy M, Nasr A, Abd-Alhaseeb M, Swidan S. (2018). Design, optimization and characterization of a transfersomal gel using miconazole nitrate for the treatment of candida skin infections. *Pharmaceutics* 10:26.
- Rajagopalan R, Hiemenz PC. 1997. *Principles of colloid and surface chemistry*. 3rd ed. New York: Marcel Dekker.
- Raval A, Bahadur P, Raval A. 2017. Effect of nonionic surfactants in release media on accelerated in-vitro release profile of sirolimus eluting stents with biodegradable polymeric coating. *J Pharm Anal* 8:45–54.
- Ribeiro A, Sosnik A, Chiappetta DA, et al. (2012). Single and mixed poloxamine micelles as nanocarriers for solubilization and sustained release of ethoxzolamide for topical glaucoma therapy. *J R Soc Interface* 9:2059–69.
- Romero A, Grau M, Villamayor F, et al. (1996). Ocular tolerance of sertaconazole gel. *Mycoses* 39:57–60.
- Salama AH, Shamma RN. (2015). Tri/tetra-block co-polymeric nanocarriers as a potential ocular delivery system of lornoxicam: in-vitro characterization, and in-vivo estimation of corneal permeation. *Int J Pharm* 492:28–39.
- Sezgin Z, Yüksel N, Baykara T. (2006). Preparation and characterization of polymeric micelles for solubilization of poorly soluble anticancer drugs. *Eur J Pharm Biopharm* 64:261–8.
- Shubber S, Vllasaliu D, Rauch C, et al. (2015). Mechanism of mucosal permeability enhancement of CriticalSorb<sup>®</sup>(Solutol<sup>®</sup>HS15) investigated in vitro in cell cultures. *Pharm Res* 32:516–27.
- Turco Liveri ML, Licciardi M, Sciascia L, et al. (2012). Peculiar mechanism of solubilization of a sparingly water soluble drug into polymeric micelles. Kinetic and equilibrium studies. *J Phys Chem B* 116:5037–46.
- Vautier-Giongo C, Bakshi MS, Singh J, et al. (2005). Effects of interactions on the formation of mixed micelles of 1,2-diheptanoyl-sn-glycero-3-phosphocholine with sodium dodecyl sulfate and dodecyltrimethylammonium bromide. *J Colloid Interface Sci* 282:149–55.
- Wei Z, Hao J, Yuan S, et al. (2009). Paclitaxel-loaded Pluronic P123/F127 mixed polymeric micelles: formulation, optimization and in vitro characterization. *Int J Pharm* 376:176–85.
- Yan H, Song J, Zhang Z, Jia X. (2016). Optimization and anticancer activity in vitro and in vivo of baohuoside I incorporated into mixed micelles based on lecithin and Solutol HS 15. *Drug Deliv* 23:2911–18.
- Yokoyama M. (2014). Polymeric micelles as drug carriers: their lights and shadows. *J Drug Target* 22:576–83.
- Yoncheva K, Vandervoort J, Ludwig A. (2011). Development of mucoadhesive poly (lactide-co-glycolide) nanoparticles for ocular application. *Pharm Dev Technol* 16:29–35.
- Zhou T, Zhu L, Xia H, et al. (2017). Micelle carriers based on macrogol 15 hydroxystearate for ocular delivery of terbinafine hydrochloride: In vitro characterization and in vivo permeation. *Eur J Pharm Sci* 109:288–96.